

# Ground-Effect Characteristics and Centerline Pressure Distributions for a Hypersonic Configuration

Robert E. Bond\*

*University of Tennessee, Knoxville, Tennessee 37996-2210*

and

Gary J. Morris† and John L. Loth†

*West Virginia University, Morgantown, West Virginia 26506-6106*

**Aircraft that operate at hypersonic speeds must adhere to stringent aerodynamic design restrictions. Typical designs incorporate complete integration of the fuselage and propulsion system. Unfortunately, these designs tend to perform poorly at subsonic speeds and demonstrate unfavorable propulsion/aerodynamic interactions when operated in ground effect for takeoff. Significant work has been done to quantify this interaction including pressure measurements using a two-dimensional model. This paper presents basic aerodynamic coefficients and centerline lower surface-pressure distributions that were measured on a three-dimensional hypersonic configuration of the National Aero-Space Plane.**

## Nomenclature

$b$	= wing span, m
$C$	= overall model length, m
$C_D$	= drag coefficient (drag/ $q_\infty S$ )
$C_L$	= three-dimensional lift coefficient (lift/ $q_\infty S$ )
$C_l$	= two-dimensional lift coefficient (lift/ $q_\infty S$ )
$C_M$	= pitching-moment coefficient (moment/ $q_\infty S c$ )
$C_T$	= three-dimensional thrust coefficient (static thrust/ $q_\infty S$ )
$C_t$	= two-dimensional thrust coefficient (static thrust/ $q_\infty c$ )
$h$	= model height above ground plane, m
$q_\infty$	= tunnel dynamic pressure, Pa
$Re$	= Reynolds number
$S$	= planform area including wings and fuselage, m <sup>2</sup>
$x$	= chordwise position measure from model nose, m
$\alpha$	= angle of attack, deg

## Introduction

**T**HERE have been many studies into the low-speed ground-effect Characteristics of hypersonic vehicles. The general conclusion was that when these airbreathing configurations are operated in ground effect (IGE) there is a significant lift/thrust interaction. Gatlin<sup>1,2</sup> tested the Generic Hypersonic Configuration with an overall length of 2.867 m (Fig. 1) in the NASA Langley Research Center 14 × 22 ft subsonic tunnel. This model used a high-pressure ejector system for thrust generation. Testing this model at  $Re = 1.3 \times 10^6/\text{ft}$  and  $\alpha = 12^\circ$  over a range of thrust coefficients from 0.0 to 0.8, he discovered the ground effect lift loss as plotted in Fig. 2. This figure shows the lift coefficient as a function of nondimensional height above the fixed ground plane ( $h/b$ ). In the power-off configuration, these data show that the model exhibits conventional ground-effect characteristics, which is an increase in  $C_L$  with reduction in height above the ground. However, this trend reverses at high thrust power so that there is a lift reduction when the model is in close ground

proximity. In fact, when the model is operated at takeoff conditions of  $\alpha = 12^\circ$ ,  $C_T = 0.6$ , and  $h/b = 0.07$  the lift produced is approximately zero.

Gatlin and Kjerstad<sup>3</sup> performed further investigation into the power-on ground effect characteristics. They used a 2.9-m (6.5%-scale) model of the National Aerospace Plane (Fig. 3) called the Test Technique Demonstrator (TTD). The TTD was a more refined hypersonic configuration including wings, a dual-angle nose ramp, and curved upper and exhaust ramp surfaces. This model also used a high-pressure ejector system for thrust simulation and was tested in the NASA Langley Research Center 14 × 22 ft subsonic tunnel at Reynolds numbers on the order of  $1.2 \times 10^6/\text{ft}$ . Figure 4 shows the lift coefficient data that were obtained using  $\alpha = 10^\circ$ . It can clearly be seen that as the model height is reduced, at a power-on condition, the lift coefficient is significantly reduced. The characteristic worsens at increased thrust and tends to make the lift coefficient nearly the same for all thrust levels at lift-off conditions of  $\alpha = 10^\circ$ ,  $C_T = 0.6$ , and  $h/b = 0.05$ .

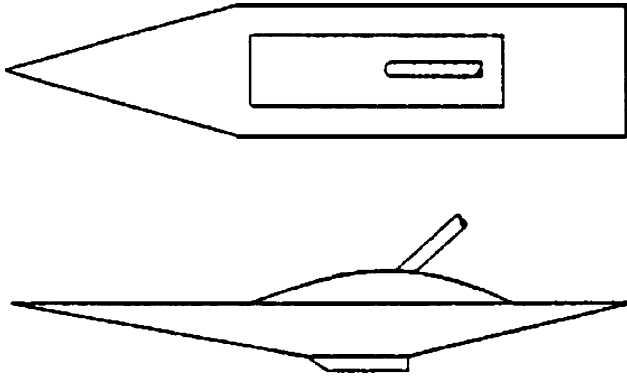
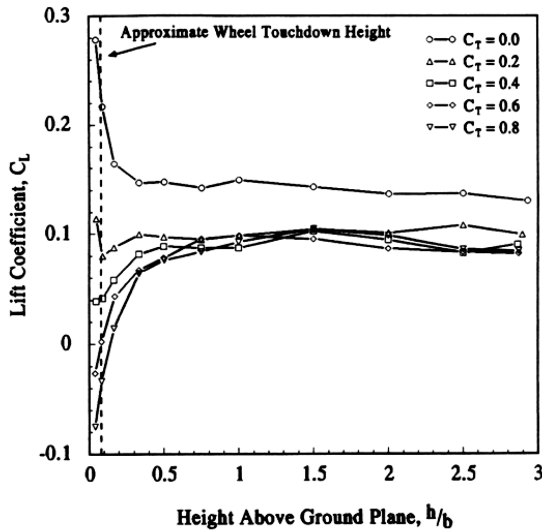
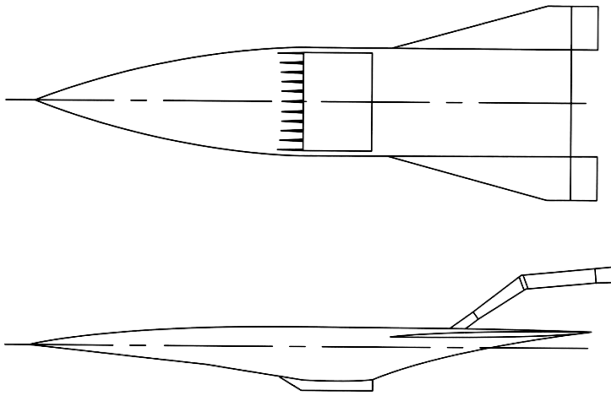
Smith<sup>4</sup> and Smith et al.<sup>5</sup> performed tests in the West Virginia University 6 × 4 ft test section using a model based on the National Aerospace Plane (NASP) Display Model, Version 2 (Refs. 6 and 7) (Fig. 5). This model had an overall length of 1.52 m (5 ft). Smith et al. showed that the lift coefficient first increased as the model was lowered from out of ground effect (OGE) to a ground proximity of  $h/b = 0.5$ . When the model was lowered further into ground effect, it demonstrated the power-on lift loss problems of the other models. These data are not shown, but they are very similar to those presented later for the current investigation.

Additional work was performed by Bond<sup>8</sup> and Bond et al.<sup>9,10</sup> using a two-dimensional configuration based on the centerline geometry of the NASP Display Model, Version 2 (Ref. 6). The two-dimensional model used a high-pressure ejector system for thrust and was equipped with pressure measurement taps along its surface. When tested IGE, at the takeoff angle of attack of  $\alpha = 10^\circ$ , this model demonstrated the characteristic ground-effect characteristics of the three-dimensional models. Figure 6 shows that without thrust there is an increase in lift coefficient when the ground spacing  $h/c$  is reduced. When the thrust coefficient was increased to higher values, this trend reversed to a strong lift loss IGE. The model surface-pressure distributions were then plotted for the highest thrust condition of  $C_t = 0.6$  with the model OGE ( $h/c = 1$ ) and at the approximate wheel touchdown height of  $h/c = 0.075$ . These data, shown in Fig. 7, clearly show the change in pressure distribution caused by the proximity of the ground plane. Highlighted on this plot are the areas of increased suction on the lower surface of the model. Based on the results of this study, it was concluded that

Received 3 February 2003; revision received 10 March 2004; accepted for publication 11 March 2004. Copyright © 2006 by the American Institute of Aeronautics and Astronautics, Inc. All rights reserved. Copies of this paper may be made for personal or internal use, on condition that the copier pay the \$10.00 per-copy fee to the Copyright Clearance Center, Inc., 222 Rosewood Drive, Danvers, MA 01923; include the code 0021-8669/06 \$10.00 in correspondence with the CCC.

\*Assistant Professor, College of Engineering, Department of Mechanical, Aerospace and Biomedical Engineering, 414 Dougherty. Member AIAA.

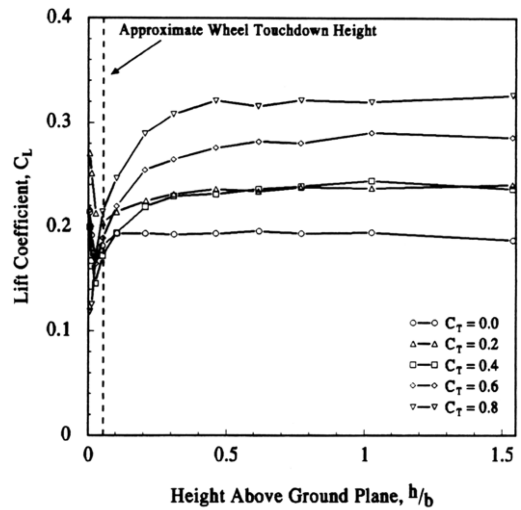
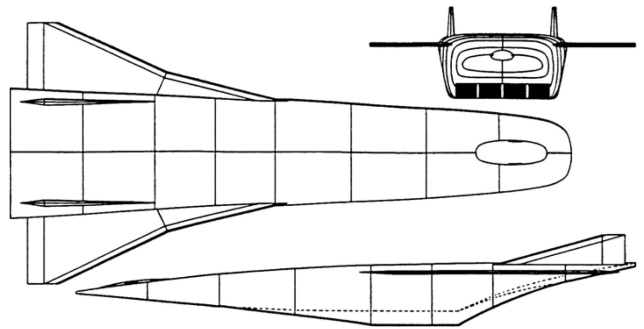
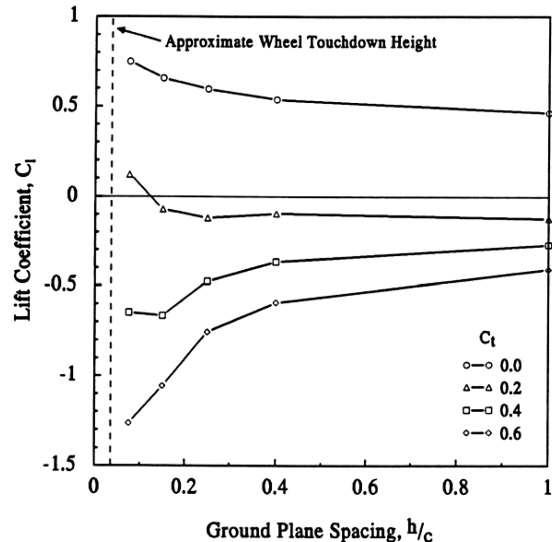
†Professor, College of Engineering and Mineral Resources, Department of Mechanical and Aerospace Engineering. Member AIAA.

Fig. 1 Generic hypersonic configuration.<sup>2</sup>Fig. 2 Effect of  $h/b$  on  $C_L$  for  $GHC^2$  ( $\alpha = 12$  deg, various  $C_T$ ).Fig. 3 Test technique demonstrator.<sup>3</sup>

model pressure distributions allowed for the identification of the single expansion ramp nozzle as the region primarily responsible for the ground-effect lift loss characteristic.

### Experimental Apparatus

Experimental tests for this research were run in the West Virginia University 4 ft  $\times$  6 ft low-speed test section. This test section has provisions for the placement of a fixed ground plane ranging from touching the model lower surface to an approximate 0.5-m spacing depending on model angle of attack. OGE data were acquired with the ground plane completely removed to minimize wall effects. For these tests, the tunnel was operated at a dynamic pressure of  $q = 200$  Pa (4.18 lb/ft<sup>2</sup>) for a Reynolds number of  $Re = 1.7 \times 10^6$  based on overall model length  $C$ .

Fig. 4 Effect of  $h/b$  on  $C_L$  for NASP TTD<sup>3</sup> ( $\alpha = 10$  deg, various  $C_T$ ).Fig. 5 NASP schematic.<sup>7</sup>Fig. 6 Effect of  $h/c$  on  $C_L$  for two-dimensional configuration<sup>8</sup> ( $\alpha = 10$  deg,  $C_T = 0.6$ ).

The model used for this work was based on the NASP Display Model, Version 2 (Ref. 6) and before modification was tested by Smith et al.<sup>4,5</sup> It was constructed from a fiberglass shell with an internal ejector system for thrust simulation. The basic dimensions were 1) wing span  $b = 71.1$  cm (28 in.), 2) total planform area including fuselage  $S = 0.545$  m<sup>2</sup> (5.87 ft<sup>2</sup>), and 3) overall model length  $C = 1.52$  m (5 ft).

The model was mounted using a three-component force measuring balance attached to the upper surface of the fuselage at

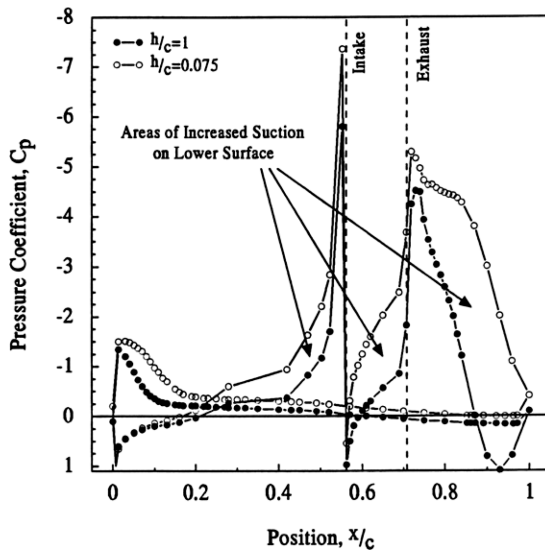


Fig. 7 Comparison of  $C_p$  distribution for  $h/c = 1$  and  $h/c = 0.075$ , two-dimensional configuration<sup>8</sup> ( $\alpha = 10$  deg,  $C_T = 0.6$ ).

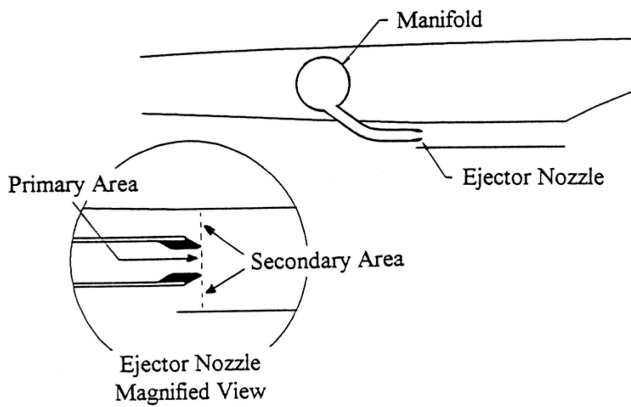


Fig. 8 Model cross section showing ejector system and flow areas.

approximately  $C/4$ . Although this placement caused significant disturbances along the upper surface, it was used to minimize adverse effects on the primary area of interest, lower portion of the model. It was also designed to allow for testing with the wings removed. This way the ground-effect aerodynamic/thrust interactions could be more easily observed without the masking effects of the wing. The same model reference area/total model planform area of the wings and fuselage was used with the wings on and off so that aerodynamic and thrust coefficients would be consistent for the different model configurations.

Model thrust was accomplished by using a high-pressure ejector system located in the model nacelle (Fig. 8). This system was powered by eight choked nozzles each with a throat diameter of 5.3 mm (0.209 in.) that yields a total primary area of  $1.77 \text{ cm}^2$  ( $0.274 \text{ in.}^2$ ). These nozzles were located near the inlet of the nacelle, which was used as a constant-area mixing chamber and gave a secondary flow area of  $103 \text{ cm}^2$  ( $16.0 \text{ in.}^2$ ) for a primary to secondary area ratio of 0.0171. The primary air was supplied from a large capacity high-pressure tank through a system that bridged the force balance without affecting the force readings. The system was calibrated by taking experimental data for the static thrust ( $q_\infty = 0$ ) as a function of the supplied manifold pressure. Figure 9 shows experimental data that were acquired plotted along with the final linear calibration curve. During model testing, the calibration was used to set the desired thrust coefficient during tunnel operation as defined by

$$C_T = T_{\text{static}}/q_\infty S$$

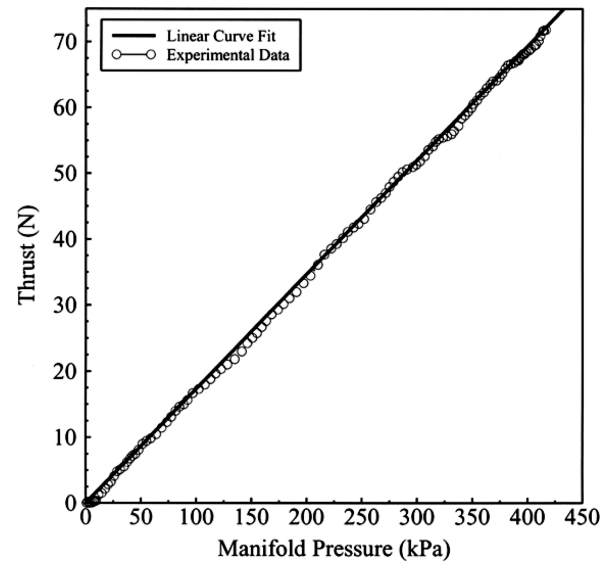


Fig. 9 Static thrust vs manifold pressure for ejector system.

The experimental error for this project was estimated using the accuracy of the various measurement systems. Evaluation of the force measuring balance showed an accuracy of  $\pm 0.7\%$  F.S. for lift,  $\pm 3.5\%$  F.S. pitching moment, and  $\pm 5.0\%$  F.S. for drag with a full-scale value of 533 N (120  $\text{lb}_f$ ), 108 Nm (80  $\text{ft} \cdot \text{lb}_f$ ) and 67N (15  $\text{lb}_f$ ), respectively. When converted to coefficient form using typical test conditions from these experiments, these values correspond to  $\Delta C_L \approx \pm 0.025$ ,  $\Delta C_m \approx \pm 0.02$ , and  $\Delta C_D \approx \pm 0.03$ . The pressure measurements were taken using a Scanivalve PDCR22 transducer with a full-scale range of 1 psid. This device was calibrated prior to every test and has an accuracy of  $\pm 0.06\%$  F.S., which corresponds to an error of  $\Delta C_p \approx \pm 0.02$  for the experimental test conditions.

## Experimental Results

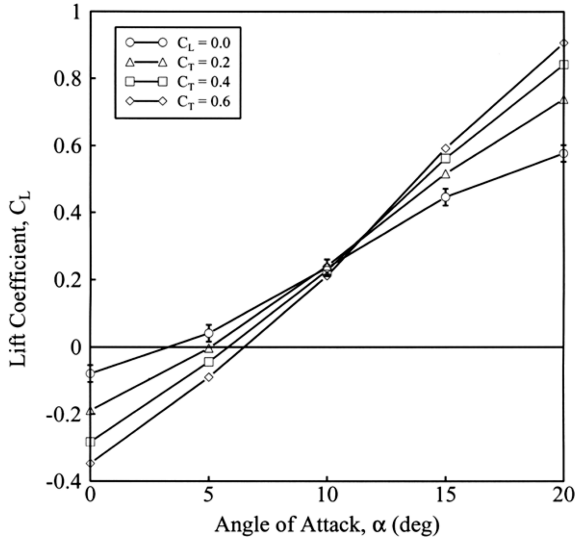
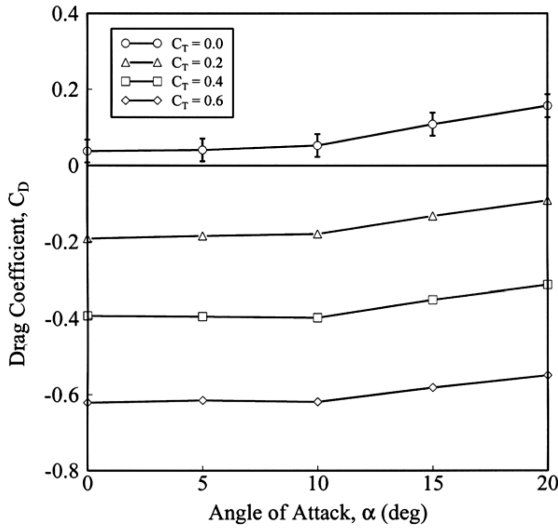
The results of this investigation were obtained at the maximum obtainable Reynolds number of  $Re = 1.7 \times 10^6$  based on overall model length. Although this value is orders of magnitude lower than that of the flight vehicle at takeoff and landing conditions, it is comparable to the Reynolds numbers used in the literature for similar studies.

The coefficient data presented herein are uncorrected values. As such, they have not been corrected for tunnel blockage, wall effects, support structure interference, or to model the actual Reynolds number of a flight vehicle.

## Out-of-Ground-Effect Data

Before investigating the ground-effect characteristics of the model, OGE data were acquired. The first parameter explored was the lift coefficient as a function of angle of attack and thrust coefficient. These data are presented in Fig. 10. The zero-thrust ( $C_T = 0.0$ ) curve shows error bars that are representative of all of the lift coefficient data acquired. Close inspection of this figure shows a slight S bend in the data; however, lift-curve slopes were assigned to each of these data sets using a linear curve fit. It is evident that the lift-curve slope increases with increasing thrust coefficient from  $dC_L/d\alpha = 1.97$  ( $0.0334/\text{deg}$ ) for  $C_T = 0.0$  to  $dC_L/d\alpha = 3.66$  ( $0.0638/\text{deg}$ ) for  $C_T = 0.6$ . The thrust-on curves ( $C_T > 0$ ) intersect at approximately  $C_L = 0.32$  and  $\alpha = 11$  deg, where the zero-thrust curve falls below this intersection at  $\alpha = 11$  deg. Although no additional data exist on this characteristic, it is believed to be because of the effective thrust line being at an 11-deg down angle with the aircraft. This would mean that at  $\alpha = 11$  deg the effective thrust would be aligned with the freestream and therefore not contribute to overall model lift.

Before presenting the drag coefficient data, it is important to discuss the measurement of these data. The drag coefficient data are a

Fig. 10 Out-of-ground effect  $C_L$  vs  $\alpha$ .Fig. 11 Out-of-ground effect  $C_D$  vs  $\alpha$ .

combination of the drag and thrust. As such, negative drag coefficients are realized when the thrust exceeds the aerodynamic drag. This can be seen in Fig. 11 along with the error bars applied to the zero-thrust condition. Here all of the curves differ approximately by the change in thrust coefficient. These curves are very similar in shape, with minimum drag occurring at  $\alpha = 0$  deg and maximum values at  $\alpha = 20$  deg. When the model is operated at zero angle of attack and a thrust coefficient of 0.6, the drag coefficient is slightly less than  $-0.6$ . As the aerodynamic drag cannot be less than zero, this indicates that the actual thrust, including interference effects, must be slightly higher than the static thrust that was used to define the thrust coefficient.

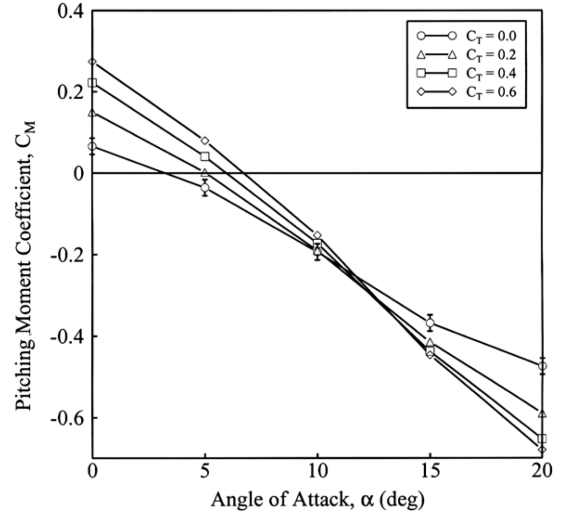
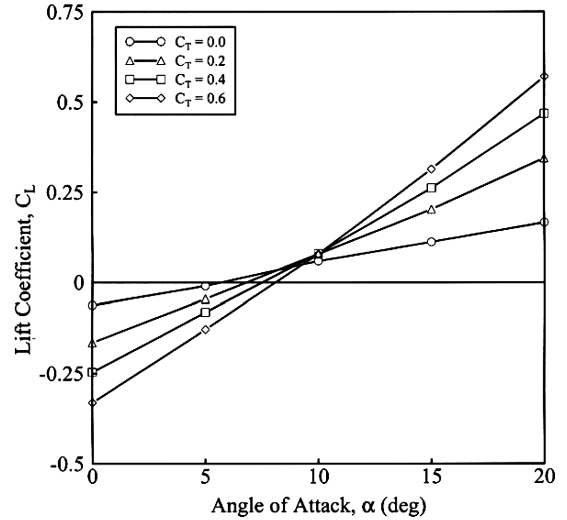
Pitching moment data obtained from these tests are presented in Fig. 12. These data are referenced to a point located at the fuselage quarter-chord ( $C/4$ ). The negative slope of these curves indicates positive static stability, and the addition of thrust increases the stability. Furthermore, all of the curves intersect at  $\alpha \approx 11$  deg.

Having quantified the basic aerodynamic performance of the baseline NASP configuration, the wings were removed and the tests repeated. Recall that the coefficients presented for this configuration are based on the baseline planform area including the wing planform area.

The trends of the lift with  $\alpha$  and  $C_T$  are similar with or without the wings. The primary differences are that the lift is greatly reduced and the lift-curve slopes are lower with the wings removed. Tabulated

Table 1 Lift-curve slopes for model operating out of ground effect

$C_T$	$dC_L/d\alpha$	
	Wing installed	Wing removed
0.0	1.97	0.67
0.2	2.72	1.45
0.4	3.27	2.03
0.6	3.66	2.57

Fig. 12 Out-of-ground effect  $C_m$  vs  $\alpha$ .Fig. 13 Out-of-ground effect  $C_L$  vs  $\alpha$  for fuselage only (no wings).

values for the lift-curve slopes are shown in Table 1. The intersection of the lift curves when thrust is applied also changes to  $C_L \approx 0.08$  at  $\alpha \approx 10$  deg (see Fig. 13).

To better demonstrate the effect of the wings, the lift coefficient data were plotted for both configurations at zero thrust and maximum thrust ( $C_T = 0.6$ ) in Fig. 14. Examination of these data clearly shows the negligible effect of the wings at zero angle of attack, which would be expected. As the angle of attack increases, the wings have an increasing effect, eventually increasing the lift coefficient by  $\Delta C_L = 0.41$  at  $C_T = 0.0$  and  $\Delta C_L = 0.34$  at  $C_T = 0.6$  at the maximum angle of attack of 20 deg. Based on these results, it can be seen that the wing has greater effect at high angles of attack, as expected, and at low thrust levels. However, when the centerline pressure data are plotted with and without the wings at  $\alpha = 20$  deg and maximum thrust coefficient (Fig. 15) there is very little difference in the data. No error bars appear on this figure as the error is on the order of the symbol size.

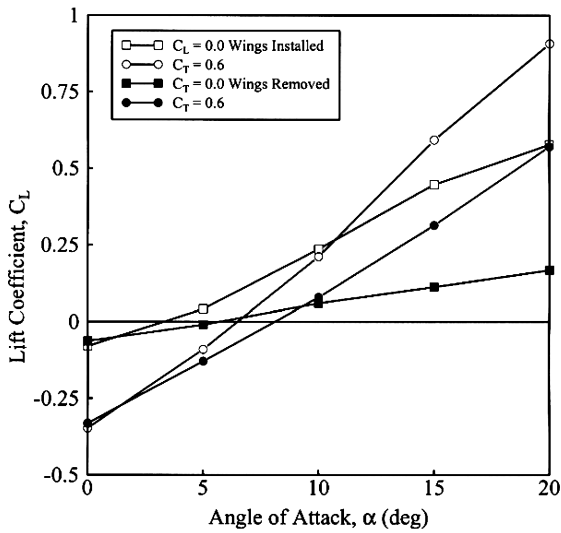


Fig. 14 Out-of-ground effect  $C_L$  vs  $\alpha$  fuselage with and without wings installed.

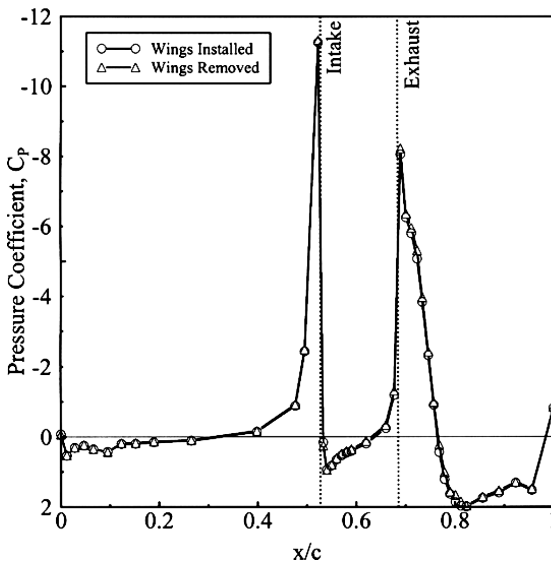


Fig. 15 Lower surface-pressure distribution ( $\alpha = 20$  deg,  $C_D = 0.6$ ).

Removing the wings had very little effect on the drag as a function of angle of attack, and so these data are not presented. The pitching-moment data showed significant effect of the wings. When comparing the data for the wings in place (Fig. 12) with Fig. 16 for the wings removed, it is clear that the wings contribute significantly to the moment data. This behavior would be expected, as the quarter-chord of the mean aerodynamic chord of the wings is located well behind the measured moment center.

### Ground-Effect Data

Once the OGE data had been acquired, the ground plane was installed and the ground-effect characteristics studied. Data acquired at the takeoff representative angle of attack of 10 deg are presented in this paper.

The lift coefficient as a function of nondimensional ground plane spacing is shown in Fig. 17 at various thrust coefficients. In this figure the OGE data are shown as  $h/b = 1.0$ , which is the approximate value that would be obtained if the lower tunnel wall were considered the ground plane. For reference, the vertical dashed line shows the location of the approximate wheel touchdown height of  $h/b = 0.07$ . From this figure it can be seen that all of the thrust coefficient curves show an increase in lift coefficient from OGE to the  $h/b = 0.5$  spacing and then they all fall as the model is lowered

Table 2 Total and percent change in lift coefficient from out-of-ground-effect to touchdown height with  $\alpha = 10$  deg

$C_T$	$\Delta C_L$	% change
0.0	0.002	0.8
0.2	-0.047	-19.3
0.4	-0.091	-40.0
0.6	-0.136	-64.4

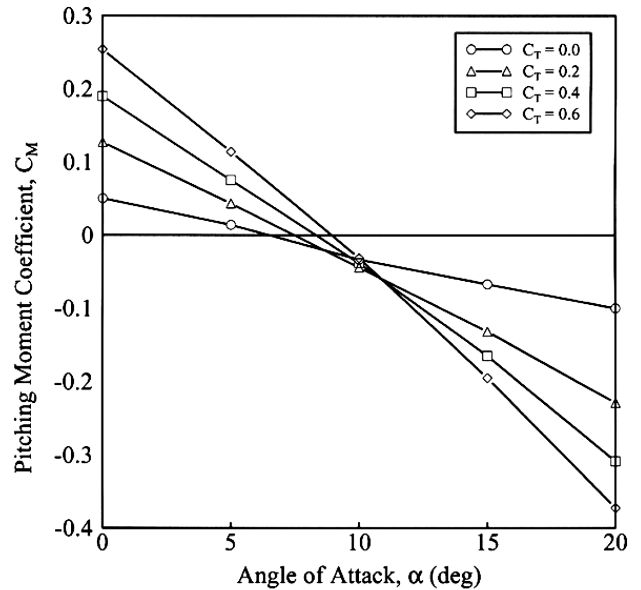


Fig. 16 Out-of-ground effect  $C_m$  vs  $\alpha$  for fuselage only (no wings).

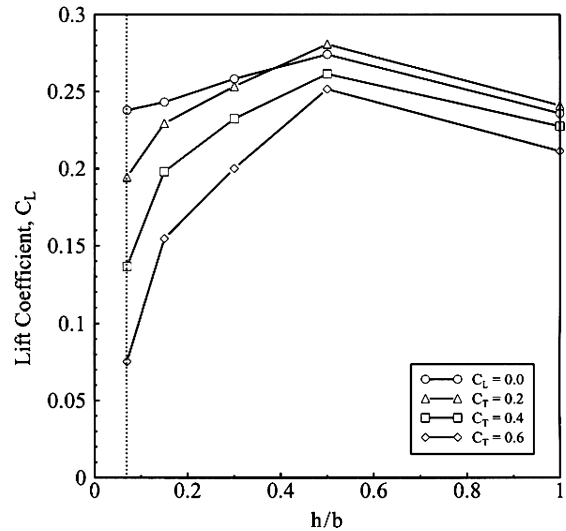


Fig. 17 Effect of ground plane spacing on lift coefficient for  $\alpha = 10$  deg.

further into ground effect. However, the curves start to diverge significantly for  $h/b$  values less than 0.5 with  $C_T = 0.6$  showing the greatest lift loss. The total change in lift coefficient and percent lift loss when the model is lowered from OGE to the touchdown representative location of  $h/b = 0.07$  is shown for each thrust coefficient in Table 2.

To further examine this ground-effect characteristic, the effect of ground plane spacing on the lower surface-pressure distribution was studied. Figure 18 shows the data for the maximum thrust coefficient of  $C_T = 0.6$  at the takeoff-representative angle of attack of  $\alpha = 10$  deg. At first glance both of these curves appear to be nearly identical contradicting the ground-effect lift loss. However, upon closer inspection it is evident that when the model is in close

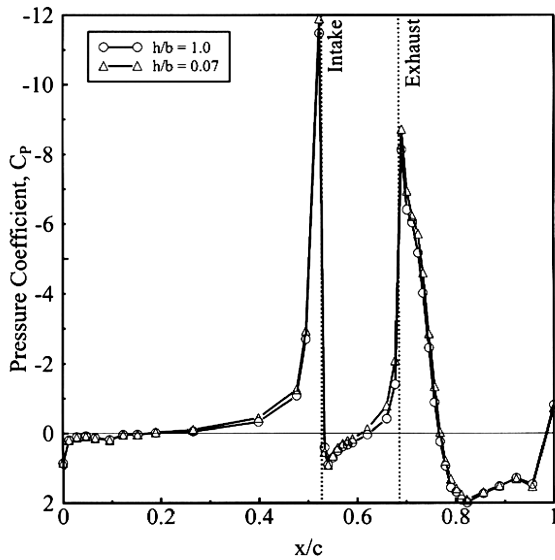


Fig. 18 In- and out-of-ground effect lower surface-pressure distribution ( $\alpha = 10$  deg,  $C_D = 0.6$ ).

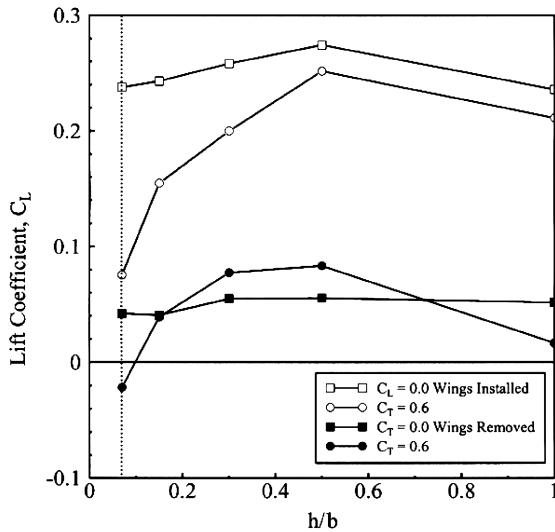


Fig. 19 Ground-effect characteristics for model with and without wings ( $\alpha = 10$  deg).

ground proximity, the lower surface pressure is somewhat lower than for the OGE condition. This small pressure change is significant enough to greatly reduce the total lift coefficient of the model. Although this curve is not as dramatic as the data Bond et al. acquired using a two-dimensional model (Fig. 7), the total lift and change in lift coefficient is much less for the three-dimensional model.

The effect that the wings have on the ground-effect lift characteristics is shown in Fig. 19. In this figure, the two higher curves were generated with the wings installed and the two lower curves with the wings removed. This greatly increased lift with the wings installed is expected and was discussed earlier. Of more interest are the ground-effect characteristics. When the model was tested with the wings removed at zero thrust, there was very little change in the

lift coefficient with ground plane spacing. However, when the thrust coefficient is increased to 0.6 the model shows similar characteristics with or without the wings. One significant difference is that when the wings are removed the lift loss in ground effect of  $\Delta C_L = -0.038$  is significantly reduced when compared to the winged model with  $\Delta C_L = -0.136$ .

## Conclusions

Experimental results obtained from this research showed similar ground-effect characteristics as those reported in the literature for hypersonic configurations with a significant lift loss when a powered model is lowered into ground effect. This trend was present with the wings installed and removed. However, removal of the wings had an almost immeasurable effect on the centerline pressure distribution.

Centerline pressure measurements taken using the three-dimensional National Aerospace Plane configuration were very similar to those reported in the literature using a two-dimensional model indicating similar flow properties. Although the pressure data were similar, the change in pressure coefficients was greatly reduced for the three-dimensional model. For this reason, a two-dimensional model is most valuable in the study of the effect of various fuselage configurations or modifications on the pressure distribution. Once the two-dimensional configuration is optimized, based on these pressure profiles, the modification could then be applied to the three-dimensional model and optimized for these flow conditions.

## Acknowledgments

The authors would like to thank the West Virginia Space Grant Consortium and the West Virginia University Department of Mechanical and Aerospace Engineering for making this research possible. We would also like to thank David Reubush at NASA Langley for serving as the contract monitor.

## References

- Gatlin, G. M., "Low-Speed Aerodynamic Characteristics of a Powered NASP-Like Configuration in Ground Effect," *Society of Automotive Engineers*, TP 892312, Sept. 1989.
- Gatlin, G. M., "Ground Effects on the Low-Speed Aerodynamics of a Powered Generic Hypersonic Configuration," NASA TP 3092, 1991.
- Gatlin, G. M., and Kjerstad, K. J., "Low-Speed Longitudinal Aerodynamic Characteristics of a Powered National Aero-Space Plane Test Technique Demonstrator Configuration in and out of Ground Effect," NASP, TP 1012, Feb. 1994.
- Smith, G., "Aerodynamic Coefficients of a Hypersonic NASP Model in Ground Effect," M.S. Thesis, West Virginia Univ., Morgantown, WV, 1996.
- Smith, G., Bond, R., Loth, J., and Morris, G., "NASP Take-Off Lift Loss Alleviation," AIAA Paper 97-0296, Jan. 1997.
- Romero, J. M., "Configuration Layout, NASP Display Model Version 2," General Dynamics, Fort Worth Div., Preliminary Design Drawing FW9010009A, Fort Worth, TX, Nov. 1990.
- Taylor, J. W. R., "National Aero-Space Plane," *Jane's All the Worlds Aircraft*, Jane's Information Group, Ltd., Alexandria, VA, 1991, 1992, pp. 455, 456.
- Bond, R. E., "Experimental and Numerical Aerodynamic Characterization of a Two-Dimensional NASP Model in Ground Effect with Thrust Simulation," Ph.D. Dissertation, West Virginia Univ., Morgantown, WV, 1997.
- Bond, R. E., Morris, G. J., and Loth, J. L., "Exhaust Ducting Effects on Takeoff Lift Loss of a Two Dimensional Hypersonic Configuration," *Journal of Aircraft*, Vol. 38, No. 2, 2001, pp. 271-276.
- Bond, R. E., Morris, G. J., and Loth, J. L., "Ground Effect Characteristics of a Two-Dimensional Hypersonic Configuration," *Journal of Aircraft*, Vol. 37, No. 3, 2000, pp. 434-439.